Long-Range Dependence and Multifractality of Ship Flow Sequences in Container Ports: A Comparison of Shanghai, Singapore, and Rotterdam

Chan-Juan Liu [1,*], **Jinran Wu** [2,*], **Harshanie Lakshika Jayetileke** [3] **and Zhi-Hua Hu** [4]

1   School of Business Administration and Customs Affairs, Shanghai Customs College, Shanghai 201204, China
2   School of Mathematical Sciences, Queensland University of Technology, Brisbane, QLD 4001, Australia
3   Department of Mathematics, Faculty of Science, University of Ruhuna, Matara 81000, Sri Lanka; harshaniejayetileke@gmail.com
4   Logistics Research Center, Shanghai Maritime University, Shanghai 201306, China; zhhu@shmtu.edu.cn
*   Correspondence: liuchanjuan@shcc.edu.cn (C.-J.L.); j73.wu@qut.edu.au (J.W.)

Abstract: The prediction of ship traffic flow is an important fundamental preparation for layout and design of ports as well as management of ship navigation. However, until now, the temporal characteristics and accurate prediction of ship flow sequence in port are rarely studied. Therefore, in this study, we investigated the presence of long-range dependence in container ship flow sequences using the Multifractal Detrended Fluctuation Analysis (MF-DFA). We considered three representative container ports in the world—including Shanghai, Singapore, and Rotterdam container ports—as the study sample, from 1 January 2013 to 31 December 2017. Empirical results suggested that the ship flow sequences are deviated from normal distribution, and the sequences with different time scales exhibited varying degrees of long-range dependence. Furthermore, the ship flow sequences possessed a multifractal nature, where the larger the time scale of ship flow time series, the stronger the multifractal characteristics are. The weekly ship flow sequence in the port of Singapore owned the highest degree of multifractality. Furthermore, the multifractality presented in the ship flow sequences of container ports are due to the correlation properties as well as the probability density function of the ship flow sequences. The study outlines the importance of adopting these features for an accurate modeling and prediction for maritime ship flow series.

Keywords: container ship traffic flow; volatility; generalized Hurst exponents; long-range dependence; multifractality

1. Introduction

The analysis of the time series characteristics of port ship flow sequences and the accurate prediction of port ship flow can provide references for the port layout design and the management of ship navigation. Port congestion has been recognized as a serious problem in all large ports in the world, which has a significant effect on the shipping date, the transportation cost, economic loss of the owner of the goods, and even the development of ports [1,2]. Nevertheless, understanding the arrival laws and accurate prediction of the port ship traffic flow are two keys to solve this problem. Therefore, this paper aims to study the arrival laws of ship traffic flow in container ports based on the long-range correlation and multifractality, and then, to provide a reference and theoretical basis for effective modeling and prediction of port ship flows.

There is an abundance of literature on long-range dependence for time series data, such as biomedical data [3–5], stock returns [6–8], hydrology [9–11], and climatology [12–14]. However, only a few studies focus on traffic flow sequences [15,16] and the research on maritime traffic flow sequences are very limited. This is mainly due to the difficulty in obtaining data on port ship traffic flow in the maritime sector. However, in recent years,

there are more and more relevant studies on the application of ship AIS data [17,18]. This makes it possible to study the time series of maritime ship flow.

Studies on maritime traffic flow, especially the ship flow sequences in the ports, are very important as they can provide basic decisions for the allocation of port operation infrastructures, rational port planning, and port investment. Furthermore, if the ship flow sequences in ports are long-range dependent and multifractal, then the traditional ships flow prediction models should revalue to incorporate this type of volatility. Unfortunately, there is no universally accepted theory to define the volatility of traffic flow sequence. In order to understand the irregular patterns of ship flow time series, especially for prediction, we need to know whether the maritime traffic flow system follows chaotic, random, or deterministic structural patterns. The complex pattern is the motivation behind the study of maritime ship flow series through the Multifractal Detrended Fluctuation Analysis (MF-DFA).

The contributions of this study are threefold: First, we present a descriptive statistics of the ship traffic flow time series. Second, we analyze the long-range dependence correlation characteristics of the ship traffic flow series using the Hurst exponent. Third, we determine the degree of multifractality of the ship traffic flow of the different ports through the Multifractal Detrended Fluctuation Analysis, and compare them based on the MF-DFA results. Our results suggested that the ship flow sequences at different time scales in the ports of Shanghai, Singapore, and Rotterdam showed different degrees of long-range dependency. Therefore, the ship flow prediction models should incorporate the long-range dependency in forecasting. In addition, the results indicated that the ship flow sequences in container ports are multifractal, where the degree of multifractality is much higher for the port of Singapore compared with Shanghai and Rotterdam.

The rest of the paper is organized as follows: Section 2 presents a brief review on the literature. Section 3 introduces the methodology used in this paper. Section 4 describes the sample data. Section 5 presents empirical results. Finally, Section 6 provides concluding observations based on the findings of the study.

2. Literature Review

In the last few decades, researchers discovered more characteristics of volatility in terms of long-range dependence and multifractality of the data in numerous fields including DNA sequences [3,4,19], climatology and hydrological time series [11,20,21], and stocks and other financial market data [6,7,22,23]. In most of these studies, the complex long-range correlations and multifractality behaviors of the time series were measured by the so called Hurst exponent, which was originally developed in hydrology for the practical matter of determining optimum dam sizing for the Nile river's volatile rain and drought conditions [22,24].

The long-range correlations can be captured using several methods, including Rescaled Range Analysis (R/S) [22], Detrended Fluctuation Analysis (DFA) [3], Wavelet analysis [25], Multifractal Detrended Fluctuation Analysis [25], and so on. Coronado et al. [26] compared various methods on Hurst exponent and pointed that DFA is superior to other methods since it is less influenced by the time series finite size than others. As a generalization of DFA, MF-DFA is a popular method for the nonstationary time series, which has been applied with great success in several areas of research. Several literatures have also demonstrated the possibility of detecting the multifractal properties in time series through MF-DFA method [9,27].

MF-DFA is a good method to study the characteristics of time series of stock market and complex traffic flow. For example, Mensi et al. [28] and Ali et al. [29] stated that MF-DFA is an acceptable choice to study comparative efficiency and the multifractality of stock markets. They found that the Islamic stock markets' adjustment to speculative activity is, in fact, higher than their conventional counterparts, and all stock market returns exhibited multifractal features. Besides, some scholars used MF-DFA to examine the highway traffic flow time series in Beijing, Shanghai and other places and discovered that the long-range

dependence behavior is ubiquitous in time series of road traffic flows. Moreover, the length of the time scale was significantly impacted on the multifractal characteristics of traffic flow sequences [30–32].

At present, a broad consensus has emerged that long-range dependence and multifractality are somewhat realistic phenomena in traffic flow series [15,33,34]. However, there is no research on the long-range correlations of the time series of maritime traffic flow. Therefore, motivated by the importance of temporal structure and long-range correlations for modeling and prediction of maritime ship flow series, we investigated the complex temporal structure and long-range correlation behaviors of the ship flow sequences of container ports from the multifractal perspective using the MF-DFA method. Evaluation of such results for container ship flow in different time scales and different container ports will facilitate the production of more insights on evolution dynamics of these ports and global trade.

3. Methodology

We analyzed the ship flow sequences of three representative container ports by the MF-DFA method, which is a generalization of DFA method [35,36]. To obtain the generalized Hurst exponent, we followed the five-step procedure introduced by [9,36] to measure the multifractality and nonstationary behavior of Brazilian rivers. Rego et al. [9] pointed out that the periodic components in the sequence should be removed at the first stage before beginning with the general procedure of Kantelhardt et al. [36].

For a record $x(i), i = 1, 2, ..., N$, where N denotes the length of the record, the MF-DFA consists of the following steps [35,36]:

Step 1: We first integrate the series and obtain the profile $y(j)$,

$$y(j) = \sum_{i=1}^{j} [x_i - \mu], \tag{1}$$

where μ is the mean value of the entire series.

Step 2: The integrated series $y(j)$ is divided into boxes of equal length s.

Step 3: In each box of length s, we calculate a polynomial fitting of $y(j)$, which represents the trend in that box. The shape of the polynomial trend is defined by the order m. A higher order m yield a more complex shape of the trend, but might lead to overfitting for a time series within small segment sizes. Therefore, in this study, we choose m equal to 2 as suggested by Ihlen (2012) [37]. The y coordinate of the fit line in each box is denoted by $y_s(j)$.

Step 4: The integrated series $y(j)$ is detrended by subtracting the local trend $y_s(j)$ in each box of length s.

Step 5: For a given box size,

$$F_q(s) = \left[\frac{1}{N} \sum_{j=1}^{N} |y(j) - y_s(j)|^q \right]^{\frac{1}{q}}. \tag{2}$$

If the series is long-range and the power-law is correlated for large values of the time scales, the fluctuation functions $F_q(s)$ can be written as Equation (3):

$$F_q(s) \sim s^{H(q)}, \tag{3}$$

where $H(q)$ is the generalized Hurst exponent. The generalized Hurst exponent $H(q)$ can be obtained by observing the slope of the log–log plots of $F_q(s)$ and scale s through the method of ordinary least squares (OLS). If $H(q)$ is independent of q, the time series is monofractal, otherwise, it is multifractal. Table 1 shows the relationship between the long-range dependence of time series and the generalized Hurst exponent.

Table 1. The relationship between the long-range dependence of time series and the generalized Hurst exponent.

Hurst Exponent	Long-Range Dependence Characteristics of Time Series
$H(q) = 0.5$	There is no long-range dependence in time series and the time series is a completely independent process.
$0.5 < H(q)$	The time series has positive long-range dependence and the overall trend in the future will be consistent with past trend.
$H(q) < 0.5$	The time series has negative long-range dependence and the overall trend in the future will be contrary to the past trend.

The value of the generalized Hurst exponent equal to 0.5 indicates an uncorrelated time series. A generalized Hurst exponent value larger than 0.5 indicates a positive long-range dependence and persistence of the series. In other words, the larger the *H* value is, the stronger the persistence is. A generalized Hurst exponent value smaller than 0.5 indicates a negative long-range dependence and antipersistence of the series. This means the closer the *H* value is to 0, the stronger the antipersistence is.

When *q* is equal to two, $H(2)$ is identical to the well-known Hurst exponent. Generally, the Hurst exponent is between 0 and 1. However, it is worth noting that the generalized Hurst index obtained by applying the MF-DFA method in this study may be greater than 1 [36,38].

The singularity spectrum $f(\alpha)$ is introduced to measure the degree of multifractality of the series and can be obtained through Legendre transform:

$$\alpha = H(q) + qH'(q), \tag{4}$$

$$f(\alpha) = q[\alpha - H(q)] + 1. \tag{5}$$

Here, α is the singularity strength and used to characterize the singularities of the time series. $f(\alpha)$ indicates the dimension of the subset of sequences that is characterized by α. The strength of multifractality can be estimated by the spans of singularity given by

$$\Delta\alpha = \alpha_{\max} - \alpha_{\min}. \tag{6}$$

4. Data

As this research investigates the long-range dependence and multifractality for ship flow sequences in container ports, we extracted required container ship flow data from the Automatic Identification System (AIS) database. The data span is from 1 January 2013 to 31 December 2017 for three representative container ports in the world—that is, Shanghai, Singapore, and Rotterdam. Figure 1 represents the original data of ship flow at different time scales for these three container ports.

The port of Shanghai is not only the largest container port in China, but also the world's largest container port. Its shipping routes reach the world's 12 largest shipping areas, and it has established business contacts with more than 500 ports in nearly 200 countries and regions. As the world's second largest container port, Singapore is also the largest transit port in the Asia-Pacific region. The Port of Rotterdam is the largest port in Europe, as well as the European Gateway. Therefore, in this study, the ports of Shanghai, Singapore, and Rotterdam were chosen to represent all the ports around the globe.

We analyzed and compared the long-range correlation and multifractality characteristics of the ship flow sequences of both Asian and European ports and the gateway ports and transit ports. In general, the ship flow sequences for the three ports depicted different characteristics at different time scales. Among them, the ship flow series of Shanghai and Rotterdam with daily and weekly time scales showed a more significant upward trend than the ship flow series of Singapore port. Ship flow sequences of the three ports with monthly scale fluctuated up and down along the time line, indicating a nonlinear

and nonstationary feature. Generally, these fluctuations are not random, but relate to the seasonal and monthly cycles.
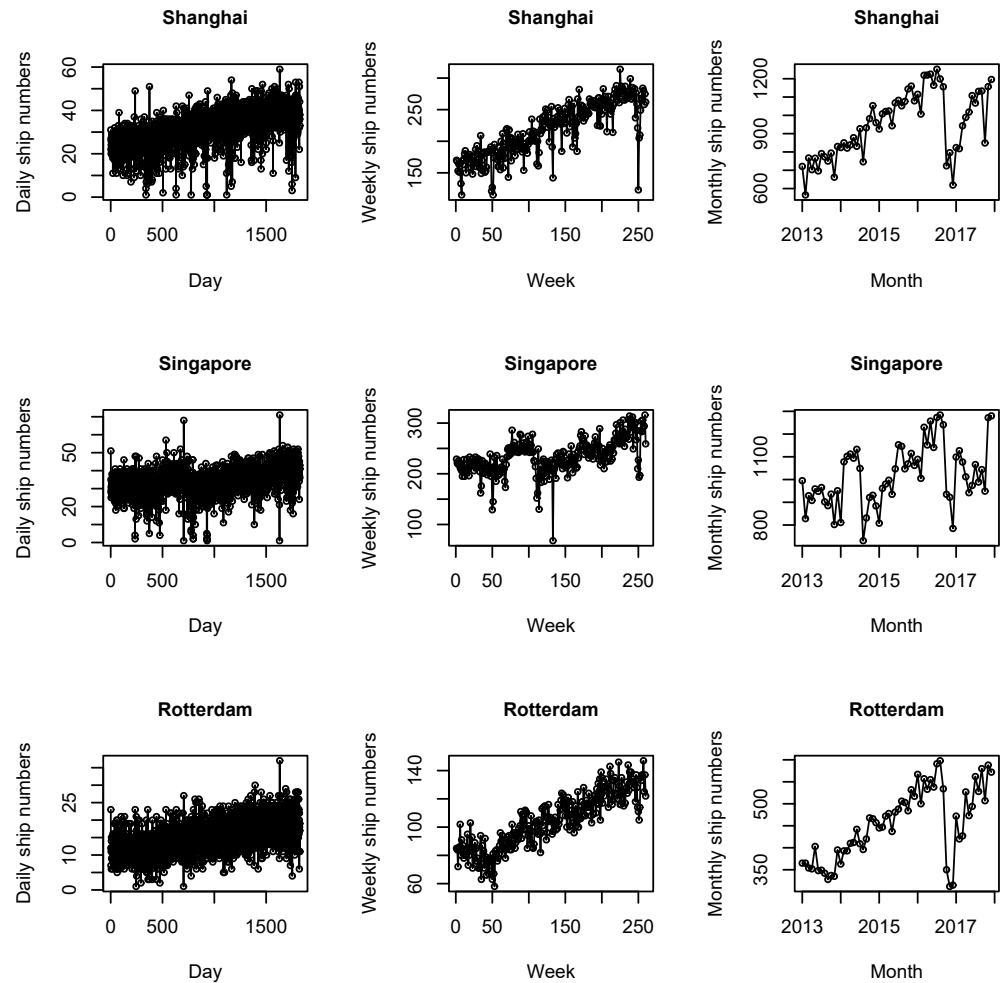

Figure 1. Original data of ship flow of different time scales in three ports.

5. Empirical Results

5.1. Descriptive Statistics

It is a well-known fact that the statistical properties of time series vary with time and depend on time windows. Table 2 presents the descriptive statistics for the original ship flow series at different time scales.

Table 2. Descriptive statistics of the original ship flow series.

Time Scale	Port	Average	Standard Deviation	Skewness	Kurtosis	ADF(p)	KPSS(p)
Daily	Shanghai	31	8.437	−0.420	0.464	−8.152(0.105)	14.418(0.01)
	Singapore	34	7.567	−0.393	2.156	−7.639(0.108)	0.598(0.01)
	Rotterdam	15	4.557	0.263	0.161	−8.989(0.290)	15.130(0.01)
Weekly	Shanghai	218	42.618	−0.177	−0.926	−4.962(0.301)	5.777(0.01)
	Singapore	235	34.244	−0.367	2.004	−3.675(0.226)	0.307(0.01)
	Rotterdam	104	19.488	−0.008	−0.820	−4.085(0.201)	6.009(0.01)
Monthly	Shanghai	950	176.878	−0.110	−1.053	−2.385(0.419)	1.443(0.01)
	Singapore	1019	134.381	0.164	−0.581	−2.684(0.299)	0.102(0.01)
	Rotterdam	453	81.193	−0.003	−1.115	−2.494(0.375)	1.640(0.01)

According to Table 2, the average number of ships arriving in the port of Singapore is greater than that of the Shanghai port at any time scale. Therefore, although Shanghai's container port ranks first in the world list, the port of Singapore is still the busiest container port in the world. This is mainly due to its unique geographical location and its role as the largest transit port in the Asia-Pacific region.

Besides, the standard deviation of ship flow sequences in port of Shanghai is larger than that of Singapore and Rotterdam ports, regardless of the time scale. This shows that the numbers of arriving ships in the ports of Rotterdam and Singapore are relatively stable compared to Shanghai.

The results from skewness and kurtosis analysis demonstrated that the different time scales significantly affect the temporal structure of the ship flow sequence. Indeed, skewness reflects the degree of symmetry in the distribution. Table 2 shows that the skewness in almost all the ship flow sequences are negative, except for the daily ship flow sequence of Rotterdam (0.263) and monthly ship flow sequence of Singapore (0.164). This indicates that all of the ship flow sequences are leftward distributions, except for the daily ship flow sequence of Rotterdam and monthly ship flow sequence of Singapore.

On the other hand, the kurtosis reflects the sharpness of the image. The higher the kurtosis, the sharper the center point on the image; in this sense, the kurtosis measures the degree of data aggregation in the center. In this study, the traditional kurtosis is replaced by the "super kurtosis" calculation method, which is to subtract the kurtosis 3 of the normal distribution from the original kurtosis so that the comparison benchmark is zero. Table 2 shows that the super kurtosis values of daily ship flow sequences are greater than 0, indicating that the daily ship flow sequence distributions are more concentrated and have a longer tail than the normal distribution. In the weekly ship flow sequences, only the super kurtosis of Singapore is greater than 0. The super kurtosis of all the monthly ship flow sequences are less than 0, indicating that these sequences are scattered and have a shorter tail than the normal distribution. Therefore, only the daily ship flow sequence of three ports and the weekly ship flow sequence of Singapore exhibited the characteristic of "sharp peak or fat tail". Further, the ship flow sequences of three ports with different time scales deviated from the normal distribution. The results are further validated by the frequency and probability density distribution of ship flow at the port in Figures 2–4.

In addition, we investigated the stationarity of the above ship flow series with different time scales. In general, the ADF and KPSS tests are complementarily used to evaluate the stationarity in time series models. Therefore, both methods were used in this study to test the stationarity of the ship flow time series with the intention of obtaining more precise results. The null hypothesis of the ADF test was the presence of a unit root, indicating the nonstationarity; the null hypothesis of the KPSS test was the absence of unit root, indicating stability. Table 1 showed that the p values of the ADF test of all the ship flow sequences were greater than 0.05; so, the null hypothesis is accepted—that is, the sequences are nonstationary time series. Similarly, the KPSS test results indicated a p value less than 0.05, rejecting the null hypothesis. Therefore, all the ship flow sequences of three ports are nonstationary time series.
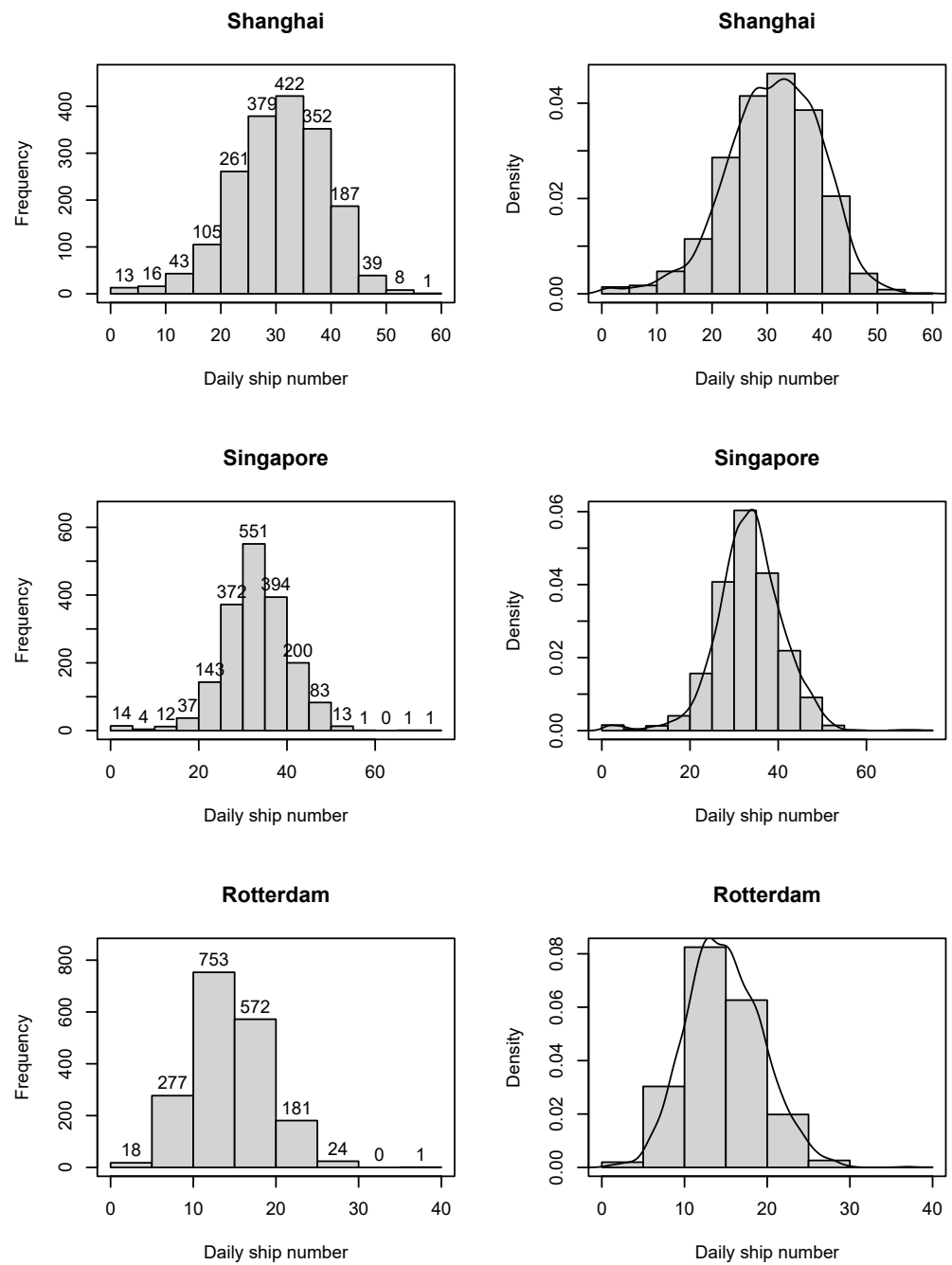
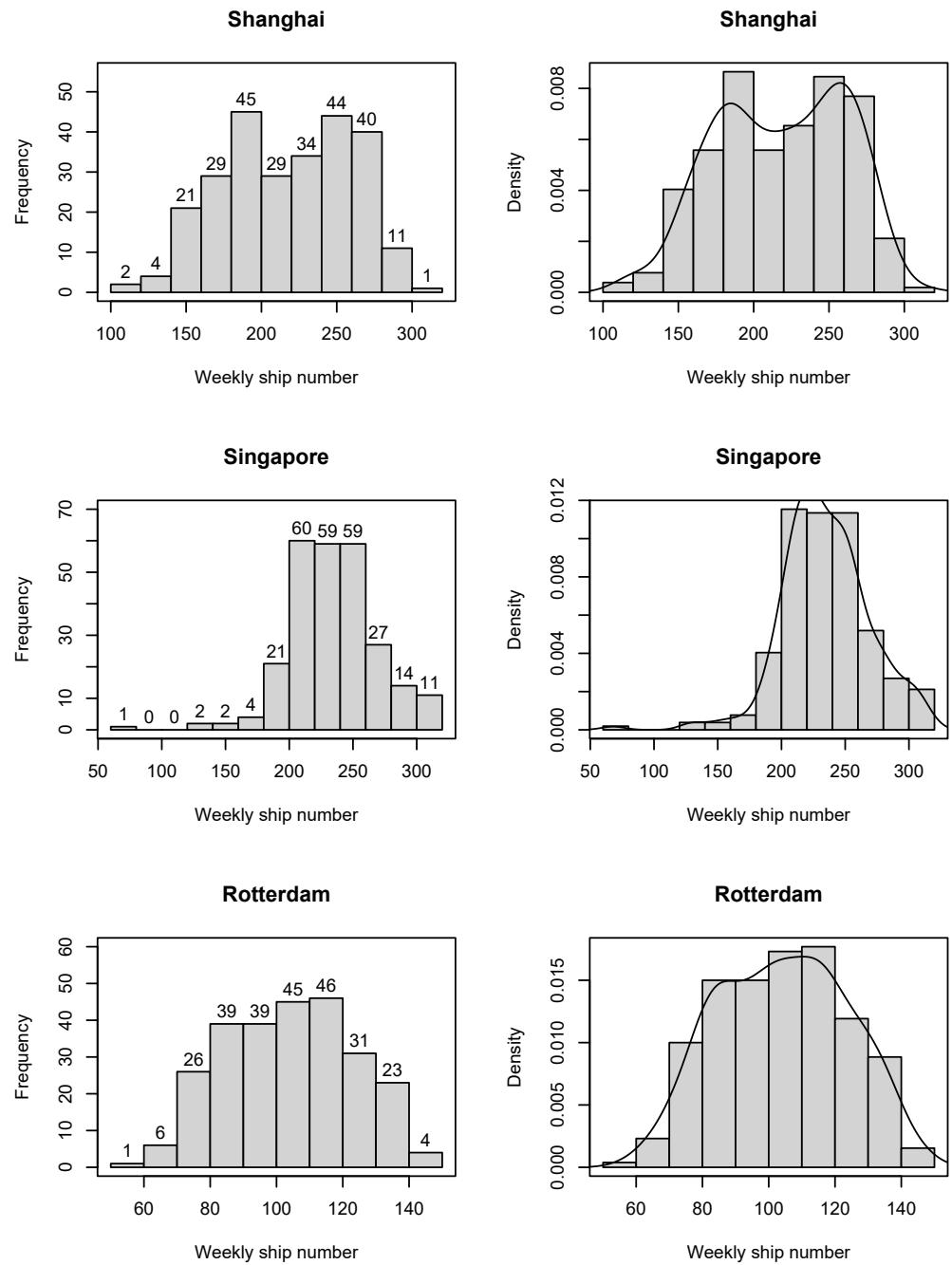**Figure 2.** Frequency and probability density distribution of daily ship flow sequences.

Figure 3. Frequency and probability density distribution of weekly ship flow sequences.
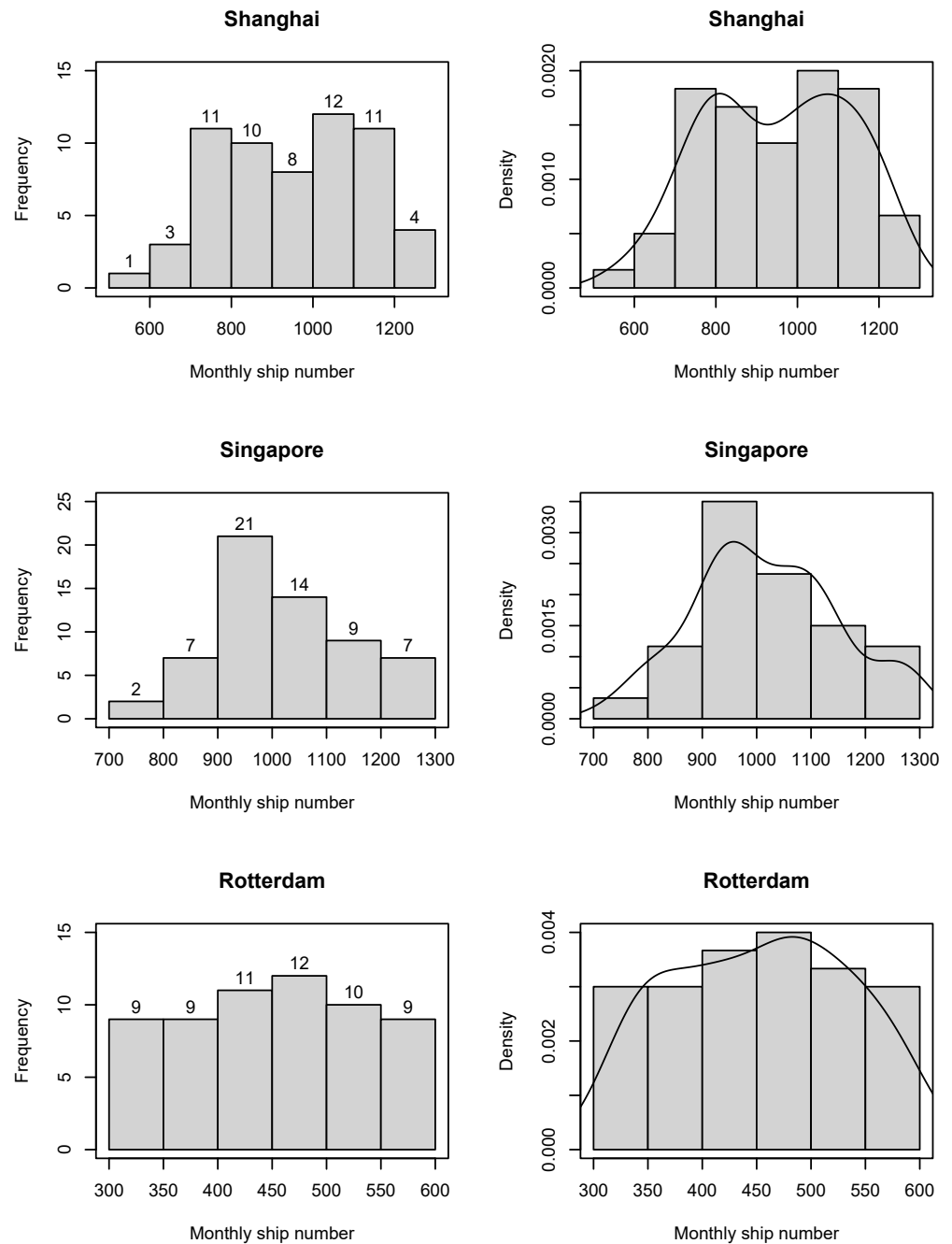
Figure 4. Frequency and probability density distribution of monthly ship flow sequences.

5.2. Long-Range Dependence and Multifractality

Figure 5 depicts the fluctuation function *F* versus scale for the ship flow sequences of three ports with different time scales in log-coordinates and the OLS linear regression for these curves when *q* is equal to two. We calculated the generalized Hurst exponents from the slopes of these straight lines. The Hurst exponent of all the ship flow sequences was greater than 0.5, which indicated a positive long-range dependence and persistence in these ship flow sequences.
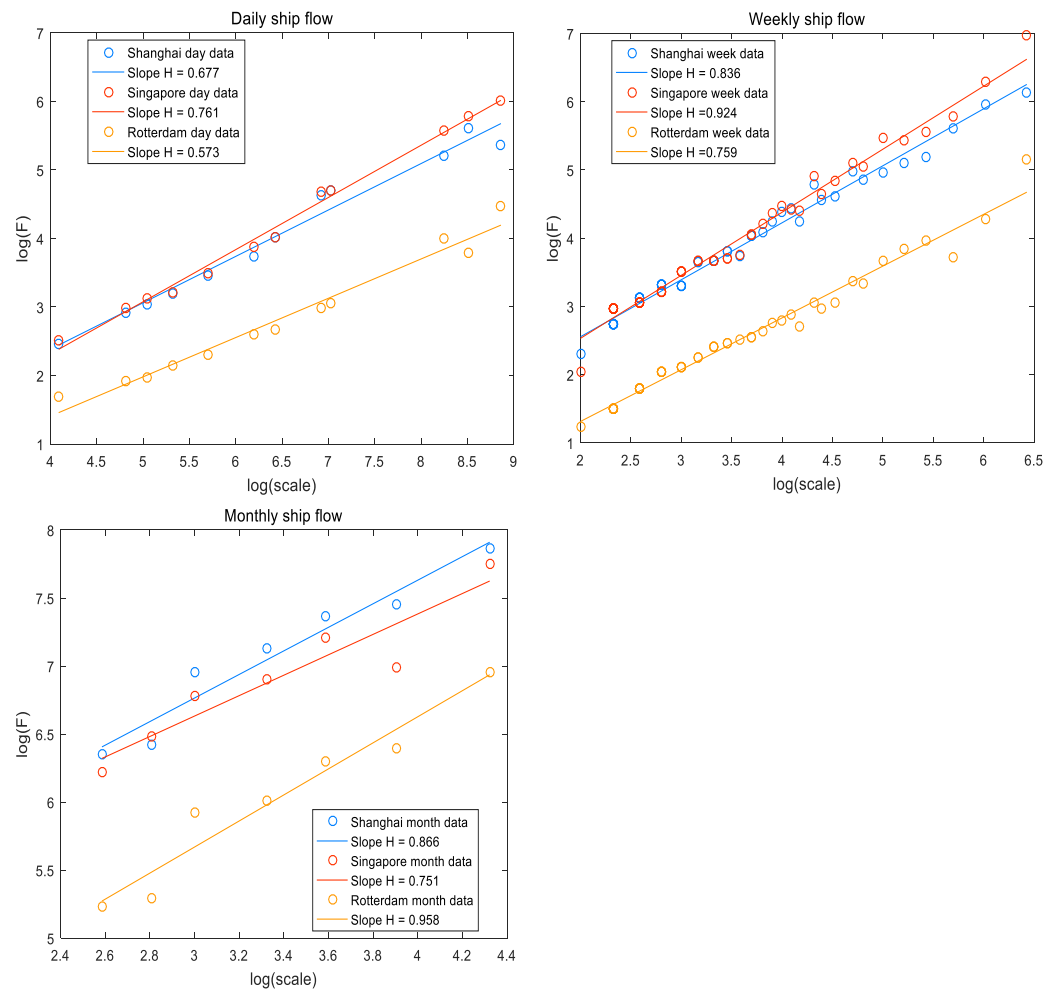
Figure 5. Generalized Hurst exponent ($q = 2$) for three ports with different time scales.

Table 3 presents the results for long-range dependence in ship flow sequences of three ports when q is equal to two. Empirical results suggested high Hurst exponents for ship flow sequences. An important feature of these results implied that, in general, Hurst exponents becomes larger as the time scale increases. The port of Singapore has the highest Hurst exponent in weekly ship flow sequence, which is close to 1. However, in the monthly ship flow sequences, Singapore obtains the lowest Hurst exponent, which is just 0.751. Therefore, ship flow sequences in the port of Singapore have a higher Hurst exponent when the time scale is small. On the contrary, the ship flow sequences in the ports of Shanghai and Rotterdam have a higher Hurst exponent when the time scale is larger. Moreover, the differences in Hurst exponents under different time scales seem to be higher for the port of Singapore.

Table 3. Generalized Hurst exponents ($q = 2$) for ship flow sequences with different time scales.

Ship Flow Sequences	Time Scale		
	Daily	**Weekly**	**Monthly**
Shanghai ($m = 2$)	0.677	0.836	0.866
Singapore ($m = 2$)	0.761	0.924	0.751
Rotterdam ($m = 2$)	0.573	0.759	0.958

Figure 6 presents the results for the MF-DFA methodology for $q = [-10 : 10]$. Qualitative results showed that the generalized Hurst exponent for all ship flow sequences decreased with the increase in q; the generalized Hurst exponent of these ship flow sequences is dependent on the selection of q. However, for the monthly ship flow sequence

in the ports of Shanghai and Rotterdam, this dependence on q was not significant. The differences in generalized Hurst exponents of daily and weekly series for three ports seem to be smaller as q increases. The generalized Hurst exponents for port of Singapore decreased faster than those for Shanghai and Rotterdam with the increase in q in all time scales. In particular, there was no substantial change in generalized Hurst exponent of the monthly ship flow series for Shanghai and Rotterdam; $H(q)$ remained between 0.8 and 1.2 with the increase in q. For the monthly sequence, when q is less than zero, the generalized Hurst exponents of Singapore and Rotterdam are larger than that of Shanghai; meanwhile, when q is larger than zero, the situation may change to the opposite, and the generalized Hurst exponent of ship flow for Shanghai becomes the largest. These results suggest that these differences are not spurious or due to error measures. An important additional comment is that the degrees of multifractality of ship flow sequences in Shanghai and Singapore container ports are much higher than the ones found for ship flow in Rotterdam port.
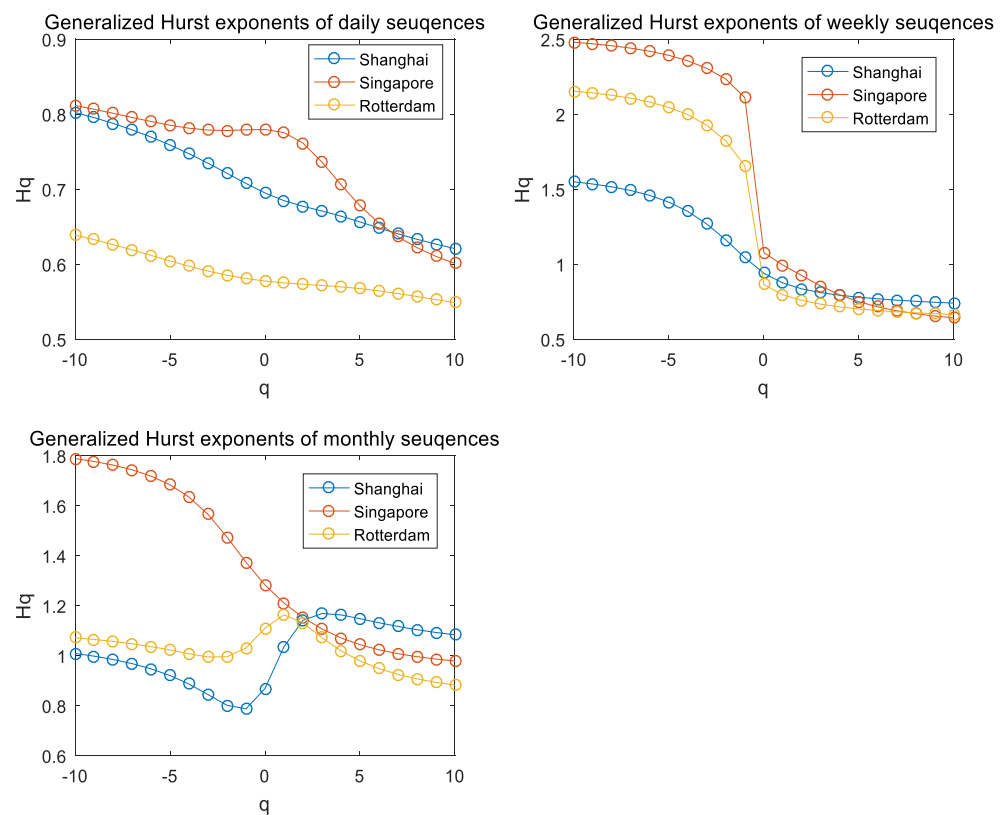

Figure 6. Hurst exponents of ship flow sequences calculated by Multifractal Detrended Fluctuation Analysis (MF-DFA) for $q = [-10 : 10]$.

The leveling of q-order Hurst exponent reflects that the q-order root-mean-square (RMS) is insensitive to the magnitude of local fluctuations. The multifractal spectrum will have a long left tail when the time series have a multifractal structure that is insensitive to the local fluctuations with small magnitudes. In contrary, the multifractal spectrum will have a long right tail when the time series have a multifractal structure that is insensitive to the local fluctuations with small magnitudes [37].

Figure 7 depicts the multifractal spectrum for ship flow sequences of three ports with different time scales. According to Figure 7, the multifractal spectrum of ship flow sequences for all ports can be divided into two sections. However, the spans of the multifractal singularity are different, implying that they have different multifractality strengths. For the daily ship flow sequences, the port of Rotterdam has the lowest multifractal strength, while the port of Singapore has the highest multifractal strength. Furthermore, the shape of multifractal spectrum of daily ship flow for Singapore shifts to the right and the spectrum is

slightly right-skewed, indicating that the scaling behavior of small fluctuations dominates the fluctuation of the daily ship flow for Singapore port.
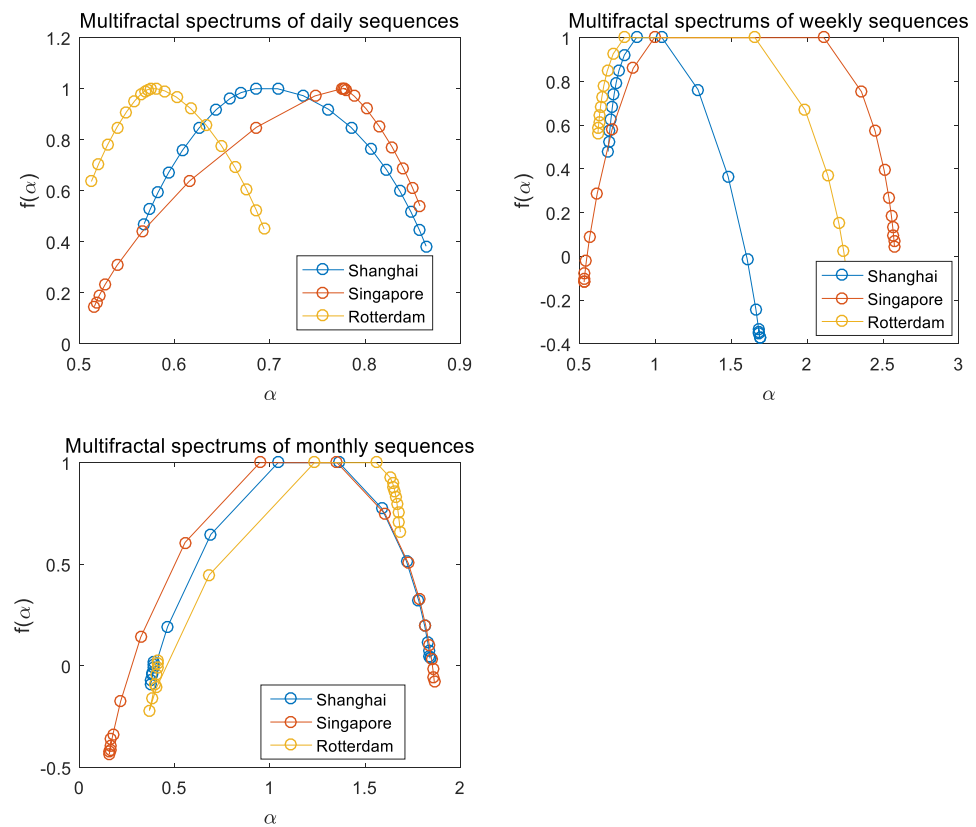

Figure 7. Multifractal spectra for ship flow sequences of three ports with different time scales.

Compared with the daily ship flow time series, the multifractal spectra of Shanghai and Rotterdam obtained from weekly ship flow sequences shifted to the left and the spectrum is slightly left-skewed. This indicates that the scaling behavior of large fluctuations dominates the fluctuation of the weekly ship flow for Shanghai and Rotterdam port.

According to the multifractal theory, the strength of multifractality can be characterized by the span of the multifractal singularity strength function in Equation (6). The bigger the $\Delta\alpha$ is, the stronger the degree of multifractality becomes.

Table 4 presents the quantitative strength of multifractality of all the ship flow sequences of the three ports. It can be seen that the degree of multifractality of weekly series is the strongest for all three ports, followed by the monthly time series, and the daily time series has the weakest multifractality. The monthly ship flow sequence of Singapore port has the highest degree of multifractality. An interpretation for this result is that the weekly ship flow sequence of Singapore is very sensitive to the changes of various influencing factors, and it is very hard to predict. Therefore, compared with the forecast of the ship traffic flows of days and months, the weekly forecast is the most difficult for the ship flow at the container port. This shows that the multifractal method is essential for the analysis of ship flow sequences.

Table 4. The strength of multifractality for ship flow sequences.

Ship Flow Sequences	Time Scale		
	Daily	**Weekly**	**Monthly**
Shanghai	0.296	0.999	0.459
Singapore	0.342	2.004	0.984
Rotterdam	0.182	1.643	0.383

5.3. Type of Multifractality

Another contribution of this study is to identify the type of multifractality presented in the ship traffic flow data. We performed the same analysis on the randomly shuffled series of the original ship traffic flow sequences. The randomly shuffled sequences were obtained by shuffling the original ship flow sequences. The shuffled sequences remained with the same fluctuation distributions, though it destroyed any temporal correlations in the original data.

The process of shuffling can be depicted as the three steps presented by [39]. Firstly, (p, q) pairs are generated from random integer numbers with $p, q \leq N$, where N is the length of the original time series. Secondly, p and q entries are swapped with each other. Finally, the above two steps are repeated $N = 20$ times to ensure that the original series is fully shuffled.

We shuffled the ship flow sequences and calculated $H_{\text{shuffle}}(q)$. As seen in Figure 8, the $H_{\text{shuffle}}(q)$ is approximately 0.5 for most of the ship flow sequences except for the weekly ship flow sequences of Singapore. The shuffled ship flow sequences with $H_{\text{shuffle}}(q)$ of about 0.5, indicating the multifractality of these ship flow sequences, are caused by different fluctuations in correlations of small and large scales. However, the multifractality of the weekly ship flow sequences of Singapore port is caused by a broadening of the probability density function. This result is consistent with the results shown in Figure 3. Therefore, the multifractality presented in the ship flow sequences of container ports are due to the correlation properties as well as the probability density function of the ship flow series.
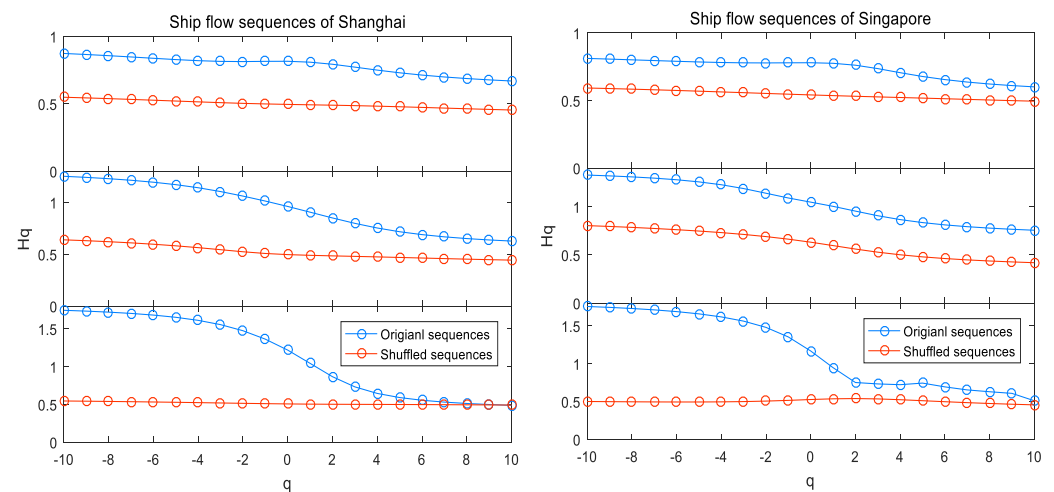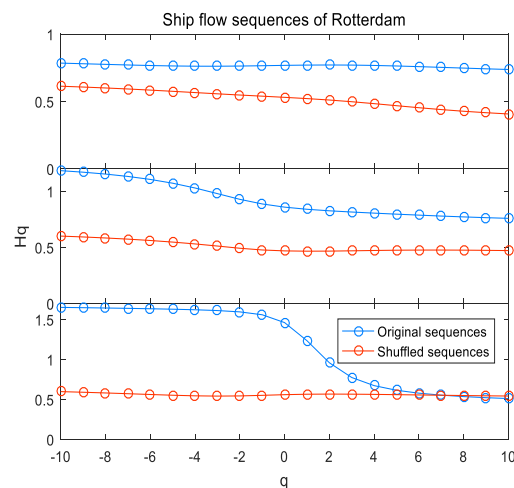

Figure 8. *Cont.*

Figure 8. Hurst exponents of the shuffled ship flow sequences for $q = [-10 : 10]$.

6. Conclusions

In this study, we investigated the statistical properties of container ship flow time series and made a detailed investigation on long-range behaviors and fractal characteristics of ship flow sequences for three representative container ports in the world—Shanghai, Singapore, and Rotterdam. This study concludes three main findings.

Firstly, the empirical evidence given in this study emphasize the significance of long-range dependence behaviors and multifractal property in all ship flow sequences at different time scales for three container ports.

Secondly, the empirical evidence from comparisons among these ship flow sequences at different time scales implies that the long-range dependence becomes larger for each port as the time scale increases, except for the port of Singapore. Shanghai and Rotterdam were identified as the ports with the highest degree of long-range dependence in monthly ship flow sequences, while Singapore was identified as having the highest degree of long-range dependence in weekly ship flow sequence.

Finally, the empirical evidence confirmed the multifractal property as an impact factor on the ship flow sequences of container ports. The analysis on the shuffled data indicated that the presence of multifractality in the ship flow sequences of container ports is due to the correlation properties as well as to the probability density function of the ship flow series.

The findings of this study provide some interesting implications. First, the existence of long-range dependence and multifractality in container ship flow could be exploitable and helpful for shipping companies and policy makers. In other words, the presence of chaotic structure such as long-range dependence and multifractality in container ship flow sequences implies that the volume and direction of container ship flow may demand certain rules. Therefore, the shipping company can carry out short-term capacity allocation and adjustment according to container ship flow prediction. Second, the presence of long-range dependence and multifractality in the data suggests that container ship flow forecasting models should account for existing nonlinearities in the data, otherwise, their results may be biased and highly misleading.

Port groups can use these findings in forecasting the expected volatility in the number of arriving container ships, and thereby, in developing and carrying out the layout planning of the port infrastructure, shipping date planning, and even port expansion investment. Moreover, some advanced modeling approaches can be employed for ship flow sequence forecasting, such as statistical modeling [40,41] and machine learning methods [42,43].

In addition, we regarded the trends in the ship traffic flow time series in this study as caused by external conditions. We identified and filtered out these trends in MF-DFA analysis. However, these trends may not be completely caused by external conditions, and some trends may carry endogenous power from data. At this time, when we explore the long-range power-law dependence of the time series, whether to filter out the trend

needs further discussion, as pointed out by Hu et al. [38]. The effect of trends on detrended fluctuation analysis for ship traffic flow time series of ports can be further studied in the future.

Author Contributions: C.-J.L.: conceptualization, methodology, software, validation, formal analysis, investigation, visualization; J.W.: writing—review and editing; H.L.J.: writing—review and editing; Z.-H.H.; resources, data curation, writing—original draft preparation, supervision. All authors have read and agreed to the published version of the manuscript.

Institutional Review Board Statement: Not applicable.

Informed Consent Statement: Not applicable.

Data Availability Statement: The data used to support the findings of this study are available from the corresponding author upon reasonable request.

Conflicts of Interest: The authors declare no conflict of interest.

References

1. Simões, P.; Marques, R.C. Influence of congestion efficiency on the European seaports performance: Does it matter? *Transp. Rev.* **2010**, *30*, 517–539. [CrossRef]
2. Ke, G.Y.; Li, K.W.; Hipel, K.W. An integrated multiple criteria preference ranking approach to the Canadian west coast port congestion conflict. *Expert Syst. Appl.* **2012**, *39*, 9181–9190. [CrossRef]
3. Peng, C.K.; Buldyrev, S.V.; Havlin, S.; Simons, M.; Stanley, H.E.; Goldberger, A.L. Mosaic organization of DNA nucleotides. *Phys. Rev. E* **1994**, *49*, 1685. [CrossRef] [PubMed]
4. Audit, B.; Vaillant, C.; Arneodo, A.; d'Aubenton Carafa, Y.; Thermes, C. Long-range correlations between DNA bending sites: Relation to the structure and dynamics of nucleosomes. *J. Mol. Biol.* **2002**, *316*, 903–918. [CrossRef]
5. Leite, A.; Rocha, A.; Silva, M.; Gouveia, S.; Carvalho, J.; Costa, O. Long-range dependence in heart rate variability data: ARFIMA modelling vs. detrended fluctuation analysis. In Proceedings of the 2007 Computers in Cardiology, Durham, NC, USA, 30 September–3 October 2007; IEEE: Piscataway, NJ, USA, 2007; pp. 21–24.
6. Cajueiro, D.O.; Tabak, B.M. Evidence of long range dependence in Asian equity markets: The role of liquidity and market restrictions. *Phys. A Stat. Mech. Appl.* **2004**, *342*, 656–664. [CrossRef]
7. Mishra, R.K.; Sehgal, S.; Bhanumurthy, N. A search for long-range dependence and chaotic structure in Indian stock market. *Rev. Financ. Econ.* **2011**, *20*, 96–104. [CrossRef]
8. Pérez-Rodríguez, J.V.; Andrada-Félix, J.; Rachinger, H. Testing the forward volatility unbiasedness hypothesis in exchange rates under long-range dependence. *N. Am. J. Econ. Finance* **2021**, *57*, 101438. [CrossRef]
9. Rego, C.; Frota, H.; Gusmão, M. Multifractality of Brazilian rivers. *J. Hydrol.* **2013**, *495*, 208–215. [CrossRef]
10. Tyralis, H.; Dimitriadis, P.; Koutsoyiannis, D.; O'Connell, P.E.; Tzouka, K.; Iliopoulou, T. On the long-range dependence properties of annual precipitation using a global network of instrumental measurements. *Adv. Water Resour.* **2018**, *111*, 301–318. [CrossRef]
11. Iliopoulou, T.; Papalexiou, S.M.; Markonis, Y.; Koutsoyiannis, D. Revisiting long-range dependence in annual precipitation. *J. Hydrol.* **2018**, *556*, 891–900. [CrossRef]
12. Pal, S.; Dutta, S.; Nasrin, T.; Chattopadhyay, S. Hurst exponent approach through rescaled range analysis to study the time series of summer monsoon rainfall over northeast India. *Theor. Appl. Climatol.* **2020**, *142*, 581–587. [CrossRef]
13. Karmakar, S.; Goswami, S.; Chattopadhyay, S. Exploring the pre-and summer-monsoon surface air temperature over eastern India using Shannon entropy and temporal Hurst exponents through rescaled range analysis. *Atmos. Res.* **2019**, *217*, 57–62. [CrossRef]
14. Chakraborty, S.; Chattopadhyay, S. Exploring the Indian summer monsoon rainfall through multifractal detrended fluctuation analysis and the principle of entropy maximization. *Earth Sci. Inform.* **2021**, *14*, 1571–1577. [CrossRef]
15. Chand, S.; Aouad, G.; Dixit, V.V. Long-Range Dependence of Traffic Flow and Speed of a Motorway: Dynamics and Correlation with Historical Incidents. *Transp. Res. Rec.* **2017**, *2616*, 49–57. [CrossRef]
16. Wang, J.L.; Wei, H.R.; Ye, C.; Ding, Y. Fractal behavior of traffic volume on urban expressway through adaptive fractal analysis. *Phys. A Stat. Mech. Appl.* **2016**, *443*, 518–525.
17. Hu, Z.H.; Liu, C.J.; Chen, W.; Wang, Y.G.; Wei, C. Maritime convection and fluctuation between Vietnam and China: A data-driven study. *Res. Transp. Bus. Manag.* **2020**, *34*, 100414. [CrossRef]
18. Hu, Z.H.; Liu, C.J.; Tae-Woo Lee, P. Analyzing interactions between Japanese ports and the Maritime Silk Road based on complex networks. *Complexity* **2020**, *2020*, 3769307. [CrossRef]

19. Ghorbani, M.; Jonckheere, E.A.; Bogdan, P. Gene expression is not random: Scaling, long-range cross-dependence, and fractal characteristics of gene regulatory networks. *Front. Physiol.* **2018**, *9*, 1446. [CrossRef] [PubMed]

20. Gaudio, R.; De Bartolo, S.G.; Primavera, L.; Gabriele, S.; Veltri, M. Lithologic control on the multifractal spectrum of river networks. *J. Hydrol.* **2006**, *327*, 365–375. [CrossRef]

21. Franzke, C. Nonlinear trends, long-range dependence, and climate noise properties of surface temperature. *J. Clim.* **2012**, *25*, 4172–4183. [CrossRef]

22. Hurst, H.E. Long-term storage capacity of reservoirs. *Trans. Am. Soc. Civ. Eng.* **1951**, *116*, 770–799. [CrossRef]

23. Wang, Z.; Yan, Y.; Chen, X. Long-range correlation and market segmentation in bond market. *Phys. A Stat. Mech. Appl.* **2017**, *482*, 477–485. [CrossRef]

24. Wang, Y.; Wei, Y.; Wu, C. Analysis of the efficiency and multifractality of gold markets based on multifractal detrended fluctuation analysis. *Phys. A Stat. Mech. Appl.* **2011**, *390*, 817–827. [CrossRef]

25. Abry, P.; Veitch, D. Wavelet analysis of long-range-dependent traffic. *IEEE Trans. Inf. Theory* **1998**, *44*, 2–15. [CrossRef]

26. Coronado, A.V.; Carpena, P. Size effects on correlation measures. *J. Biol. Phys.* **2005**, *31*, 121–133. [CrossRef] [PubMed]

27. Wang, F.; Liao, G.P.; Zhou, X.Y.; Shi, W. Multifractal detrended cross-correlation analysis for power markets. *Nonlinear Dyn.* **2013**, *72*, 353–363. [CrossRef]

28. Mensi, W.; Hamdi, A.; Yoon, S.M. Modelling multifractality and efficiency of GCC stock markets using the MF-DFA approach: A comparative analysis of global, regional and Islamic markets. *Phys. A Stat. Mech. Appl.* **2018**, *503*, 1107–1116. [CrossRef]

29. Ali, S.; Shahzad, S.J.H.; Raza, N.; Al-Yahyaee, K.H. Stock market efficiency: A comparative analysis of Islamic and conventional stock markets. *Phys. A Stat. Mech. Appl.* **2018**, *503*, 139–153. [CrossRef]

30. Shang, P.; Lu, Y.; Kamae, S. Detecting long-range correlations of traffic time series with multifractal detrended fluctuation analysis. *Chaos Solitons Fractals* **2008**, *36*, 82–90. [CrossRef]

31. Doménech-Carbó, A. Rise and fall of historic tram networks: Logistic approximation and discontinuous events. *Phys. A Stat. Mech. Appl.* **2019**, *522*, 315–323. [CrossRef]

32. Feng, S.; Wang, X.; Sun, H.; Zhang, Y.; Li, L. A better understanding of long-range temporal dependence of traffic flow time series. *Phys. A Stat. Mech. Appl.* **2018**, *492*, 639–650. [CrossRef]

33. Wang, Y.; Vormer, F.; Hu, M.; Duong, V. Empirical analysis of air traffic controller dynamics. *Transp. Res. Part C Emerg. Technol.* **2013**, *33*, 203–213. [CrossRef]

34. Yuan, P.; Lin, X. How long will the traffic flow time series keep efficacious to forecast the future? *Phys. A Stat. Mech. Appl.* **2017**, *467*, 419–431. [CrossRef]

35. Gómez-Extremera, M.; Carpena, P.; Ivanov, P.C.; Bernaola-Galván, P.A. Magnitude and sign of long-range correlated time series: Decomposition and surrogate signal generation. *Phys. Rev. E* **2016**, *93*, 042201. [CrossRef]

36. Kantelhardt, J.W.; Zschiegner, S.A.; Koscielny-Bunde, E.; Havlin, S.; Bunde, A.; Stanley, H.E. Multifractal detrended fluctuation analysis of nonstationary time series. *Phys. A Stat. Mech. Appl.* **2002**, *316*, 87–114. [CrossRef]

37. Ihlen, E.A.F. Introduction to Multifractal Detrended Fluctuation Analysis in Matlab. *Front. Physiol.* **2012**, *3*, 141. [CrossRef]

38. Hu, K.; Ivanov, P.C.; Chen, Z.; Carpena, P.; Stanley, H.E. Effect of trends on detrended fluctuation analysis. *Phys. Rev. E* **2001**, *64*, 011114. [CrossRef]

39. Lu, W.Z.; Xue, Y. Detrended fluctuation analysis of particle number concentrations on roadsides in Hong Kong. *Build. Environ.* **2014**, *82*, 580–587. [CrossRef]

40. Xu, X.; McGrory, C.A.; Wang, Y.G.; Wu, J. Influential factors on Chinese airlines' profitability and forecasting methods. *J. Air Transp. Manag.* **2021**, *91*, 101969. [CrossRef]

41. Zhang, S.; Wu, J.; Jia, Y.; Wang, Y.G.; Zhang, Y.; Duan, Q. A temporal LASSO regression model for the emergency forecasting of the suspended sediment concentrations in coastal oceans: Accuracy and interpretability. *Eng. Appl. Artif. Intell.* **2021**, *100*, 104206. [CrossRef]

42. Zhu, M.; Wu, J.; Wang, Y.G. Multi-horizon accommodation demand forecasting: A New Zealand case study. *Int. J. Tour. Res.* **2021**, *23*, 442–453. [CrossRef]

43. Wu, J.; Wang, Y.G.; Tian, Y.C.; Burrage, K.; Cao, T. Support vector regression with asymmetric loss for optimal electric load forecasting. *Energy* **2021**, *223*, 119969. [CrossRef]